

# Synthesis, Photo- and Electro-Luminescence of 3-Benzoxazol-2-yl-Coumarin Derivatives

Yuling Zhao · Tianzhi Yu · Youzhi Wu · Hui Zhang ·  
Duowang Fan · Zunwei Gan · Liangliang Yang ·  
Xiaoqian Han · Yumei Zhang

Received: 30 June 2011 / Accepted: 14 October 2011 / Published online: 19 October 2011  
© Springer Science+Business Media, LLC 2011

**Abstract** Two coumarin derivatives containing electron-transporting benzoxazolyl moiety, 7-(diethylamino)-3-(benzoxazol-2-yl)coumarin (DABOC) and 3-(benzoxazol-2-yl)benzo[5,6]coumarin (BOBC), were synthesized and characterized. The photoluminescence and electroluminescence of the compounds were investigated detailedly. The compounds exhibited strong blue-green emissions in both solution and solid states, but the devices with DABOC as the emitting layer exhibited orange emission and maximum luminous efficiency of 2.8 cd/A and maximum luminance of 8,800 cd/m<sup>2</sup>, and the devices with BOBC displayed orange-white emission and maximum luminous efficiency of 0.13 cd/A and maximum luminance of 540 cd/m<sup>2</sup>.

**Keywords** Synthesis · UV-vis Absorption · Photoluminescence · Electroluminescence · Coumarin derivative · Benzoxazolyl derivative

Y. Zhao (✉) · T. Yu · Z. Gan · L. Yang · X. Han · Y. Zhang  
School of Chemical and Biological Engineering,  
Lanzhou Jiaotong University,  
Lanzhou 730070, China  
e-mail: zhaoyl66@hotmail.com

T. Yu · H. Zhang · D. Fan  
Key Laboratory of Opto-Electronic Technology and Intelligent  
Control (Lanzhou Jiaotong University), Ministry of Education,  
Lanzhou 730070, China

Y. Wu  
School of Materials Science & Engineering,  
Lanzhou University of Technology,  
Lanzhou 730050, China

## Introduction

Organic light-emitting diodes (OLEDs) has been studied by many research groups throughout the world due to its high efficiency, low power consumption, fast response time, wide viewing angle and so on [1–4]. Organic electroluminescent (EL) devices or organic light-emitting diodes using fluorescent molecules have attracted great interest in flat-panel displays and may have the potential to replace liquid crystal technology [5–7].

Coumarin and its derivatives are well known not only for their remarkable biological and medical activities [8–10], but also for their super thermal stability and outstanding optical properties including an extended spectral response, high quantum yields, large Stokes shifts and good photostability [11–16]. Coumarin derivatives can be applied to laser dyes, fluorescent whiteners, fluorescent probes, nonlinear optical chromophores, polymer science, optical recording and solar energy collectors [17, 18]. More important, coumarin dyes were used as blue, green and red dopants in organic light-emitting diodes (OLEDs) [19–21]. Coumarin derivatives substituted at 7-position with an electron-donating group and at 3-position with an electron-withdrawing group are a typical class of D-A structure molecules and exhibit strong fluorescence [12, 22–25].

Following our interest on designing and synthesising new coumarin derivatives with high quantum yield of fluorescence and greater stability [12, 13, 22, 26–28], two coumarin derivatives with benzoxazolyl moiety, 7-(diethylamino)-3-(benzoxazol-2-yl)coumarin (DABOC) and 3-(benzoxazol-2-yl)benzo[5,6]coumarin (BOBC), were synthesized and structurally characterized in this paper. The UV-vis and emission spectra of the compounds were investigated. We fabricated the electroluminescence

devices by vacuum vapor-deposited film with the compounds as emission materials and investigated the electroluminescent properties.

## Experimental

### Materials and Methods

4-(*N,N'*-diethylamino)salicylaldehyde from Zhejiang Huadee Dyestuff Chemical Co. Ltd. (China) was recrystallized from ethanol. 2-Hydroxy-1-naphthaldehyde was obtained from Acros Organics. *Ortho*-aminophenol and ethyl cyanoacetate were purchased from AstaTech (Chengdu) Pharmaceutical Co., Ltd. All other chemicals were analytical grade reagents.

IR spectra (400–4,000  $\text{cm}^{-1}$ ) were measured on a Shimadzu IRPrestige-21 FT-IR spectrophotometer.  $^1\text{H}$  NMR spectra were obtained on Unity Varian-500 MHz. C, H, and N analyses were obtained using an Elemental Vario-EL automatic elemental analysis instrument. Melting points were determined on a X-4 microscopic melting point apparatus made in Beijing Taike Instrument Limited Company and the quoted temperatures were uncorrected. UV-vis absorption and photoluminescent spectra were recorded on a Shimadzu UV-2550 spectrometer and on a Perkin-Elmer LS-55 spectrometer, respectively. The electroluminescent spectra were measured on a PR-650 SpectraScan Colorimeter.

### Synthesis and Characterization

of 7-(Diethylamino)-3-(Benzoxazol-2-yl)Coumarin (DABOC) and 3-(Benzoxazol-2-yl)Benzo[5,6]Coumarin (BOBC)

The synthetic routes were shown in Scheme 1. 7-(diethylamino)-3-(benzoxazol-2-yl)coumarin (DABOC) was synthesized according to the method reported by Ye et al. [29]

7-(Diethylamino)-3-(Benzoxazol-2-yl)Coumarin (DABOC) Under nitrogen atmosphere, a mixture of 4-(*N,N'*-diethylamino)salicylaldehyde (3.40 g, 17.6 mmol), *Ortho*-

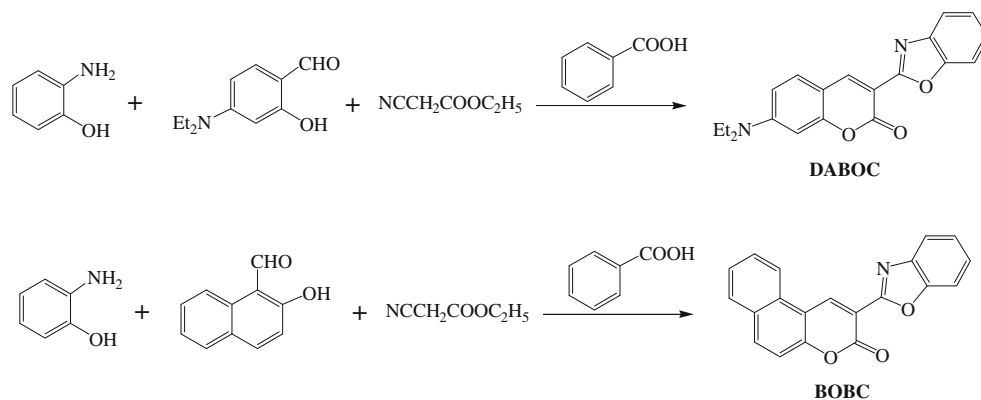
aminophenol (1.92 g, 17.6 mmol), ethyl cyanoacetate (2.00 g, 17.6 mmol) and benzoic acid (1.10 g, 8.5 mmol) was dissolved in 1-butanol (50 mL). The mixture solution was refluxed for 8 h till the reaction was completed (monitored by TLC). After the solvent was partly evaporated under reduced pressure, the reaction mixture was cooled to room temperature. 100 mL NaOH (2%) was added into the mixture and stirring about 0.5 h. The crude product was obtained by filtering and then recrystallized from methanol to afford a yellow powder. Yield: 65% (3.82 g). m. p.: 185–186  $^{\circ}\text{C}$ ; IR (KBr pellet,  $\text{cm}^{-1}$ ): 3063 (Aryl-CH), 2971, 2929, 2891 (Alkyl-CH), 1748 (C=O, lactone), 1624 (C=N), 1606 (C=C), 1588, 1508, 1451, 772, 740  $\text{cm}^{-1}$ ;  $^1\text{H}$  NMR (500 MHz,  $\text{CDCl}_3$ ,  $\delta$ , ppm): 8.65 (s, 1H, 4-H), 7.81 (t,  $J=4.8$  Hz, 1H, Aryl-H), 7.60 (t,  $J=4.4$  Hz, 1H, Aryl-H), 7.42 (d,  $J=9.2$  Hz, 1H, Aryl-H), 7.36–7.32 (m, 2H, Aryl-H), 6.66 (d,  $J=2.4$  Hz, 1H, Aryl-H), 6.54 (s, 1H, Aryl-H), 3.47 (q,  $J=7.2$  Hz, 4H, N- $\text{CH}_2$ - $\text{CH}_3$ ), 1.26 (t,  $J=7.2$  Hz, 6H, N- $\text{CH}_2$ - $\text{CH}_3$ ). Anal. Calcd. for  $\text{C}_{20}\text{H}_{18}\text{N}_2\text{O}_3$ : C, 71.84; H, 5.43; N, 8.38. Found: C, 71.81; H, 5.45; N, 8.40.

3-(Benzoxazol-2-yl)Benzo[5,6]Coumarin (BOBC) The preparation of BOBC was similar to that described for DABOC. The crude product was recrystallized from DMF to afford yellow floccules. Yield: 87%. m.p.:  $> 250$   $^{\circ}\text{C}$ . IR (KBr pellet,  $\text{cm}^{-1}$ ): 3065 (Aryl-CH), 1734 (C=O, lactone), 1624 (C=N), 1608 (C=C), 1568, 1457, 1215, 770, 736  $\text{cm}^{-1}$ ;  $^1\text{H}$  NMR (500 MHz,  $\text{CDCl}_3$ ,  $\delta$ , ppm): 9.65 (s, 1H, 4-H), 8.73 (d,  $J=8.8$  Hz, 1H, Aryl-H), 8.35 (d,  $J=9.2$  Hz, 1H, Aryl-H), 8.12 (d,  $J=8.0$  Hz, 1H, Aryl-H), 7.91–7.80 (m, 3H, Aryl-H), 7.68 (t,  $J=7.6$  Hz, 2H, Aryl-H), 7.53–7.45 (m, 2H, Aryl-H). Anal. Calcd. for  $\text{C}_{20}\text{H}_{11}\text{NO}_3$ : C, 76.67; H, 3.54; N, 4.47. Found: C, 76.71; H, 3.56; N, 4.45.

### OLEDs Fabrication

The multilayer OLEDs were fabricated by vacuum-deposition method. ITO-coated glass with a sheet resistance

**Scheme 1** Synthetic routes of 7-(diethylamino)-3-(benzoxazol-2-yl)coumarin (DABOC) and 3-(benzoxazol-2-yl)benzo[5,6]coumarin (BOBC)



$R_{\square} \sim 20 \Omega/\square$  was cut into 3 cm×3 cm plates and etched in dilute hydrochloric acid for 20 min. Then the ITO substrates were routinely cleaned by ultrasonic treatment in solvents and then cleaned by exposure to an UV-ozone ambient. All organic layers were sequentially deposited without breaking vacuum ( $2 \times 10^{-4}$  Pa). Thermal deposition rates for organic materials, LiF and Al were  $\sim 2 \text{ \AA/s}$ ,  $\sim 1 \text{ \AA/s}$  and  $10 \text{ \AA/s}$ , respectively. The active area of the devices was  $12 \text{ mm}^2$ . The EL spectra were measured on a PR-650 SpectraScan Colorimeter. The characterization of brightness-current-voltage (B–I–V) were measured with a 3645 DC power supply combined with a 1980A spot photometer and were recorded simultaneously. All measurements were done in the air at room temperature without any encapsulation.

## Results and Discussion

### Absorption and Fluorescence of DABOC and BOBC

UV-vis absorption and photoluminescent spectra of the compound DABOC and BOBC in diluted acetonitrile solutions are shown in Fig. 1. It is shown that the absorption spectrum of DABOC exhibits absorption maxima at 220, 279 and 437 nm, respectively. The absorption spectrum of BOBC is similar to that of DABOC, there are three absorption bands at 220, 260 nm and 390 nm. Compared with DABOC, the second and third absorption bands of BOBC were blue-shifted. It is suggesting that the compound DABOC has an electron repelling diethylamine in the 7-position which enhances the electron density of coumarin ring, however, the compound BOBC has a benzocoumarin skeleton which disperses the electron density of coumarin ring, so the absorption bands of BOBC were blue-shifted compared to that of DABOC.

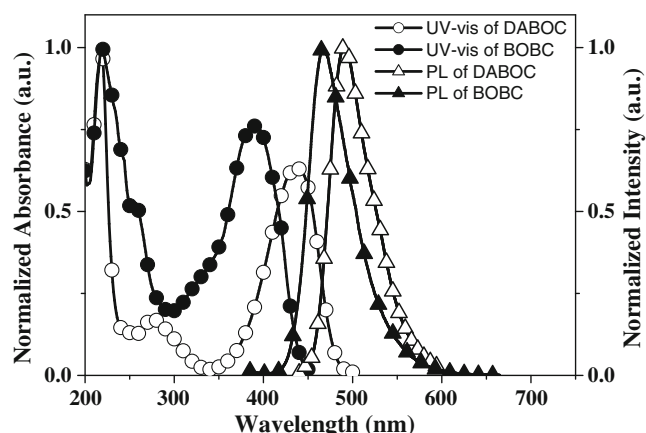


**Fig. 1** UV-vis absorption and photoluminescence spectra of DABOC and BOBC in acetonitrile solutions ( $C = 1.0 \times 10^{-6} \text{ mol/L}$ )

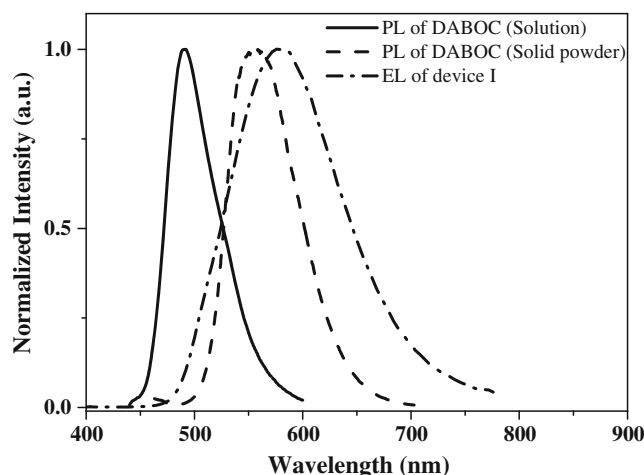


**Fig. 2** Photoluminescence spectra of DABOC in acetonitrile solution and solid powder, and electroluminescence spectrum of the device I

From Fig. 1, it is shown that the compound DABOC exhibits bright blue–green emission with peak at 490 nm and the compound BOBC shows bright blue emission at 466 nm in diluted acetonitrile solutions. The maximum emission wavelength of DABOC was bathochromically shifted by about 24 nm compared with that of BOBC due to an electron repelling diethylamine in the 7-position in DABOC molecule. From the excitation and emission maxima of DABOC and BOBC, the Stoke's shifts of DABOC and BOBC are  $2,475$  and  $4,182 \text{ cm}^{-1}$ , respectively. The compound BOBC has a larger Stoke's shift.

Fluorescence quantum yield of DABOC and BOBC in acetonitrile were measured with anthracene as reference ( $\Phi_F^S = 0.25$  [30]). The quantum yields ( $\Phi_F$ ) were calculated

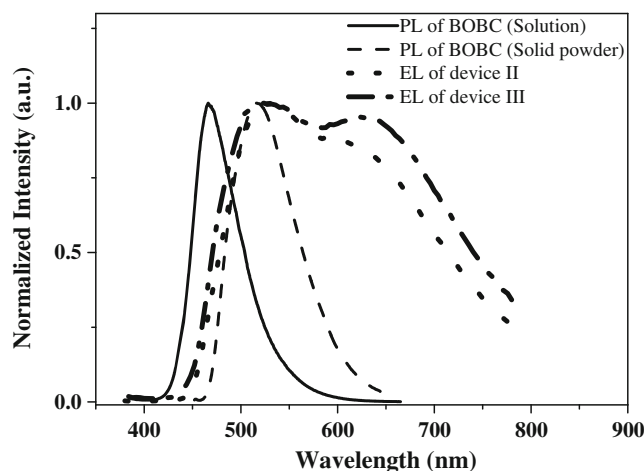
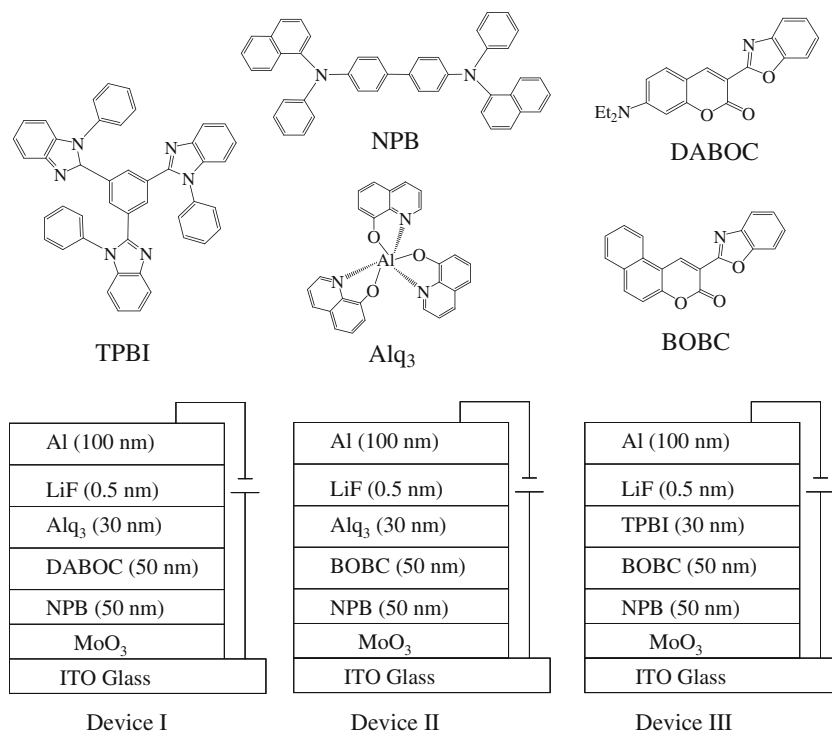


**Fig. 3** Photoluminescence spectra of BOBOC in acetonitrile solution and solid powder, and electroluminescence spectra of the device I and device III

**Fig. 4** The molecular structures of materials and the structures of EL devices

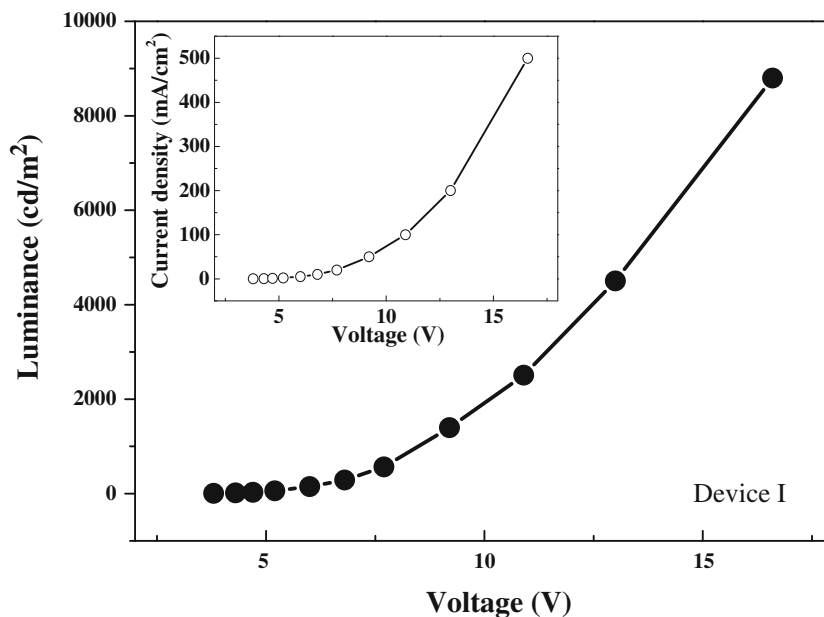


according to the literatures [30, 31]. Fluorescence quantum yields of DABOC ( $\Phi_{F, \text{DABOC}}$ ) and BOBC ( $\Phi_{F, \text{BOBC}}$ ) in acetonitrile solutions were measured to be 0.62 and 0.45, respectively.

The photoluminescence spectra of DABOC and BOBC in acetonitrile solution and solid powder were compared as shown in Figs. 2 and 3, respectively. Due to more intermolecular interaction in the solid state,

the photoluminescence spectrum of DABOC in solid powder is much broader than that in acetonitrile solution, and the emission peak is red-shifted from 490 nm in solution to 556 nm in solid powder (Fig. 2). An example of compound was reported to show such differences of PL spectra between solution and solid powder [27]. The similar phenomenon was also found in photoluminescence spectra of BOBC in acetonitrile

**Fig. 5** The luminance versus voltage and current density versus voltage (inset) curves of the device I



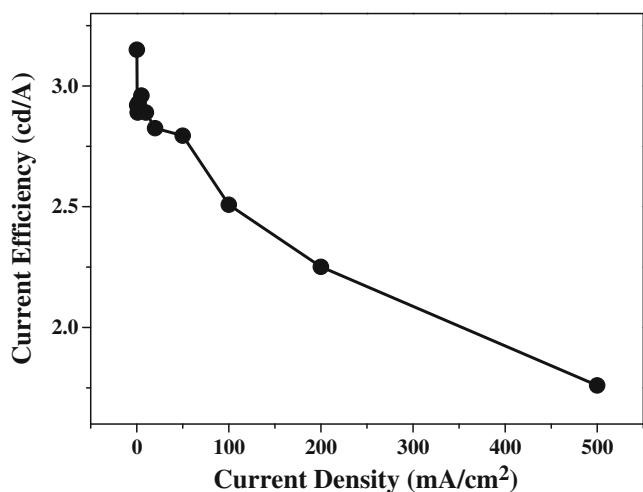


Fig. 6 Current efficiency-current density characteristic of the device I

solution and solid powder, the emission peaks of solution and solid powder appear at 466 and 518 nm, respectively (Fig. 3).

OLED Performance of DABOC and BOBC

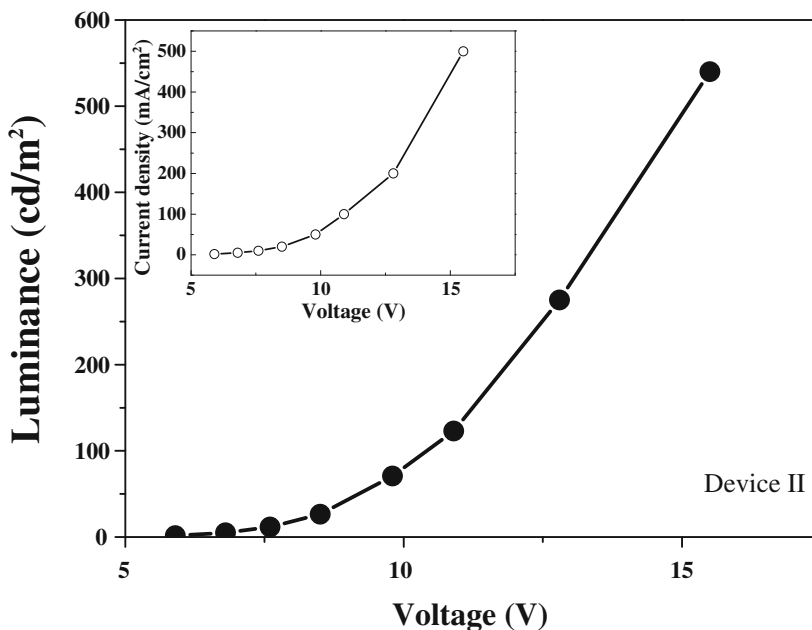
The molecular structures of the materials and the devices with the configuration of ITO / MoO<sub>3</sub> / NPB (50 nm) / DABOC (50 nm) / Alq<sub>3</sub> (30 nm) / LiF (0.5 nm) / Al (100 nm), ITO / MoO<sub>3</sub> / NPB (50 nm) / BOBC (50 nm) / Alq<sub>3</sub> (30 nm) / LiF (0.5 nm) / Al (100 nm) and ITO / MoO<sub>3</sub> / NPB (50 nm) / BOBC (50 nm) / TPBI (30 nm) / LiF (0.5 nm) / Al (100 nm) were depicted in Fig. 4. DABOC or BOBC was employed as the emitter. MoO<sub>3</sub>, NPB, and Alq<sub>3</sub> or TPBI were used as hole injection, hole transport and

electron transport materials, respectively. LiF was used as the electron-injection layer.

The EL spectrum of the device I using DABOC as emitter, as shown in Fig. 2, has an orange emission band centered at 580 nm. Compared to the photoluminescence spectrum of DABOC measured in the solid powder, the emission peak of the device I is red-shifted by 24 nm and the EL spectrum is much broader. It is well known that the EL spectrum of the device was obtained from the compact amorphous thin film while the PL spectrum of the solid powder was measured from the polycrystalline powder, the intermolecular interaction in the amorphous thin film is larger than that in solid powder of the compound, and thus it may lead to the different emission. Another reason should be reminded here that the EL spectrum was obtained from the multiple layer structures, thus some interactions may occur between NPB and DABOC and/or between DABOC and Alq<sub>3</sub> in OLEDs, yielding different PL and EL spectra.

More intriguing spectral differences between PL and EL were observed in the device II and device III containing the emitting layer of BOBC (Fig. 3). The maximum PL of BOBC in the solid powder occurred at 518 nm while the EL peaks of the device II were observed at 530 nm with a shoulder of 625 nm. Originally, the emission band at 530 nm was suspected to originate from Alq<sub>3</sub> used as electron transport material in the device II because the emission of Alq<sub>3</sub> generally appears at 530 nm. Thus, the device III with TPBI as electron transport material was fabricated, and the EL spectrum of the device III also revealed two peaks of 530 nm and 625 nm. Though the

Fig. 7 The luminance versus voltage and current density versus voltage (inset) curves of the device II



intensity of the emission at 625 nm of the device III was much larger compared to that of the device II, the EL spectra of the two devices were found to exhibit similar emitting patterns, indicating that the emission of 530 nm is attributed to the intrinsic emission from BOBC. In addition, we measured the PL spectra of the thin films of NPB and TPBI, they exhibit emission peaks at 450 nm and 385 nm, respectively. It was indicated that the emission at 625 nm of the device II or device III was originated from NPB, Alq<sub>3</sub> and TPBI. Compared to the device II, TPBI was not only used as electron transport material but also used as hole blocking layer in device III, which prohibited the holes from diffusing to TPBI layer. The results were suggested that the origin of the emission of the device II or device III at 625 nm is attributed to an exciplex formed between NPB and BOBC.

Figure 5 shows the representative luminance-current density-voltage characteristics of the device I. The turn-on voltage of the device I was observed at 4.7 V, and the maximum luminance was 8,800 cd/m<sup>2</sup> at 16.6 V. Figure 6 shows the relationship between the current efficiency and the current density in the device I. The device I exhibits a maximum luminous efficiency of 2.8 cd/A at the current density of 20 mA/cm<sup>2</sup> and the voltage of 7.7 V.

Figures 7 and 8 show the representative luminance-current density-voltage characteristics of the device II and the device III. As shown in Figs. 7 and 8, the turn-on voltages of the device II and the device III were observed at 6 V and 8 V, the maximal luminances were 540 cd/m<sup>2</sup> at 15.5 V for the device II and 170 cd/m<sup>2</sup> at 17 V for the device III. Figure 9 shows the relationships between the current efficiency and the current density in the device II

**Fig. 8** The luminance versus voltage and current density versus voltage (inset) curves of the device III

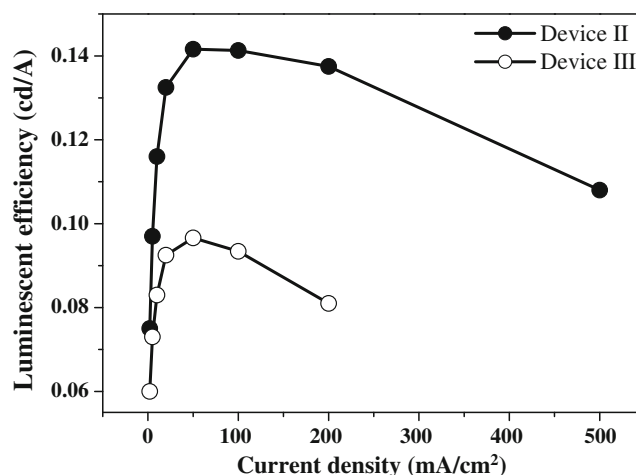
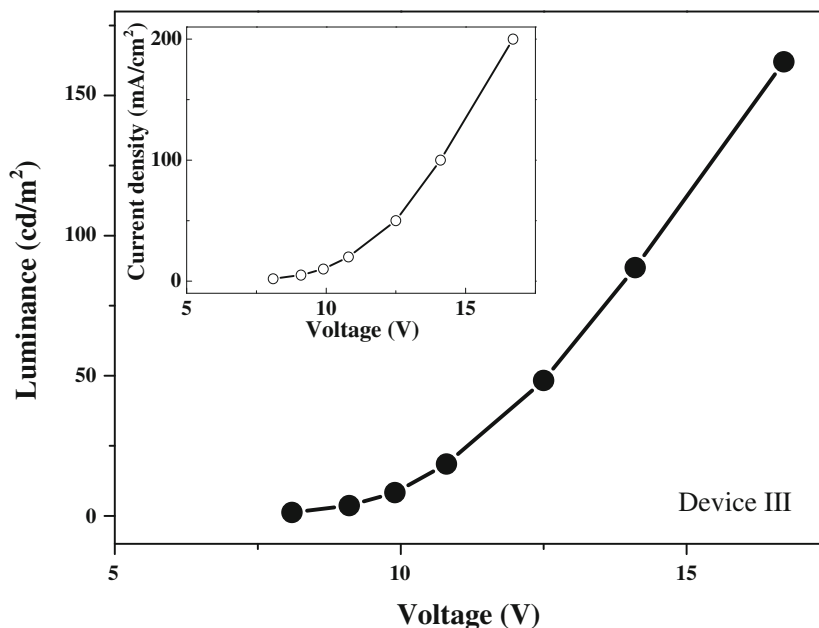


**Fig. 9** Current efficiency-current density characteristics of the device II and the device III

and the device III. The device II exhibits a maximum luminous efficiency of 0.13 cd/A at the current density of 20 mA/cm<sup>2</sup> and the voltage of 8.5 V. The device III has a maximum luminous efficiency of 0.10 cd/A at the current density of 20 mA/cm<sup>2</sup> and the voltage of 13 V. Both the devices show the orange-white emission. In terms of luminance and efficiency, the device II is much better than the device III.

To contrast the device II with the device I, although they had same structural patterns, the luminance and efficiency of the device I are much higher than that of the device II.

From the absorption spectra of DABOC and BOBC and the EL spectrum of NPB [32], it was found that the

absorption spectra of DABOC was overlapped with the EL spectrum of NPB completely while the overlap between the absorption spectra of BOBC and the EL spectrum of NPB is very small, indicating that an energy transfer from NPB to DABOC dopant could occur effectively. Namely, NPB should rather be used as host material for DABOC doped device. Further investigation on the doped device of DABOC is being carried out.

## Conclusions

We designed and synthesized two coumarin derivatives containing electron-transporting benzoxazolyl moiety, 7-(diethylamino)-3-(benzoxazol-2-yl)coumarin (DABOC) and 3-(benzoxazol-2-yl)benzo[5,6]coumarin (BOBC). The photoluminescent and electroluminescent behaviors of the compounds were investigated and discussed. Fluorescence quantum yield of DABOC is higher than that of BOBC. The devices of ITO / MoO<sub>3</sub> / NPB (50 nm) / DABOC (50 nm) / Alq<sub>3</sub> (30 nm) / LiF (0.5 nm) / Al (100 nm) displayed the orange emission (580 nm), a maximum luminous efficiency of 2.8 cd/A at the current density of 20 mA/cm<sup>2</sup>, and maximum luminance of 8,800 cd/m<sup>2</sup> at 16.6 V. The ITO / MoO<sub>3</sub> / NPB (50 nm) / BOBC (50 nm) / Alq<sub>3</sub> (30 nm) / LiF (0.5 nm) / Al (100 nm) device showed the orange-white emission (530 and 625 nm), a maximum luminous efficiency of 0.13 cd/A at the current density of 20 mA/cm<sup>2</sup>, and maximum luminance of 540 cd/m<sup>2</sup> at 15.5 V. The ITO / MoO<sub>3</sub> / NPB (50 nm) / BOBC (50 nm) / TPBI (30 nm) / LiF (0.5 nm) / Al (100 nm) device exhibited the orange-white emission (530 and 625 nm), a maximum luminous efficiency of 0.1 cd/A at the current density of 20 mA/cm<sup>2</sup>, and maximum luminance of 170 cd/m<sup>2</sup> at 17 V. In terms of luminance and efficiency, the device of DABOC is much better than the device of BOBC.

**Acknowledgements** This work was supported by the Natural Science Foundation of Gansu Province (096RJZA086) and the National Natural Science Foundation of China (Grant 60776006), and also supported by ‘Qing Lan’ talent engineering funds (QL-05-23A) by Lanzhou Jiaotong University.

## References

- Tang CW, VanSlyke SA (1987) Organic electroluminescent diodes. *Appl Phys Lett* 51:913–915
- Sheats JR, Antoniadis H, Hueschen M, Leonard W, Miller J, Moon R, Roitman D, Stocking A (1996) Organic electroluminescent devices. *Science* 273:884–888
- Friend RH, Gymer RW, Holmes AB, Burroughes JH, Marks RN, Taliani C, Bradley DDC, Dos Santos DA, Bredas JL, Lögglund M, Salaneck WR (1999) Electroluminescence in conjugated polymers. *Nature* 397:121–128
- Shinar J, Shinar R (2008) Organic light-emitting devices (OLEDs) and OLED-based chemical and biological sensors: an overview. *J Phys D: Appl Phys* 41:133001
- Li Z, Meng H (eds) (2007) Organic light-emitting materials and devices. CRC Taylor and Francis, New York
- Miller RD, Chandross EA (2010) Introduction: materials for electronics. *Chem Rev* 110:1–2
- Shinar J, Shinar R (2008) Organic light-emitting devices (OLEDs) and OLED-based chemical and biological sensors: an overview. *J Phys D: Appl Phys* 41:133001(26 pp).
- Fylaktakidou KC, Hadjipavlou-Litina DJ, Litinas KE, Nicolaides DN (2004) Natural and synthetic coumarin derivatives with anti-inflammatory / antioxidant activities. *Curr Pharm Design* 10:3813–3833
- Walshe M, Howarth J, Kelly MT, Kennedy RO, Smyth MR (1997) The preparation of a molecular imprinted polymer to 7-hydroxycoumarin and its use as a solid-phase extraction material. *J Pharm Biomed Anal* 16:319–325
- Sardari S, Mori Y, Horita K, Micetich RG, Nishibe S, Daneshalab M (1999) Synthesis and antifungal activity of coumarins and angular furanocoumarins. *Bioorg Med Chem* 7:1933–1940
- Sokolowska J, Czajkowski W, Podsiadly R (2001) The photostability of some fluorescent disperse dyes derivatives of coumarin. *Dyes Pigments* 49:187–191
- Yu TZ, Yang SD, Zhao YL, Zhang H, Han XQ, Fan DW, Qiu YQ, Chen LL (2010) Synthesis, crystal structures and fluorescence properties of 3-(2-Pyridyl)coumarin derivatives. *J Photochem Photobiol A: Chem* 214:92–99
- Zhang H, Yu TZ, Zhao YL, Fan DW, Xia YJ, Zhang P (2010) Synthesis, crystal structure, photo- and electro-luminescence of 3-(4-(anthracen-10-yl)phenyl)-7-(N, N'-diethylamino)coumarin. *Synth Met* 160:1642–1647
- Ray D, Bharadwaj PK (2008) A coumarin-derived fluorescence probe selective for magnesium. *Inorg Chem* 47:2252–2254
- Trenor SR, Shultz AR, Love BJ, Long TE (2004) Coumarins in polymers: from light harvesting to photo-cross-linkable tissue scaffolds. *Chem Rev* 104:3059–3078
- Hara K, Sayama K, Ohga Y, Shinpo A, Suga S, Arakawa H (2001) A coumarin-derivative dye sensitized nanocrystalline TiO<sub>2</sub> solar cell having a high solar-energy conversion efficiency up to 5.6%. *Chem Commun* 569–570.
- Jones G, Jackson WR, Choi C, Bergmark WR (1985) Solvent effects on emission yield and lifetime for coumarin laser dyes. Requirements for a rotatory decay mechanism. *J Phys Chem* 89:294–300
- Hiroshi T, Yoshio O, Juzo I, Masato I, Atsushi T (1990) *Jpn Kokai Tokyo Koho* (CODEN: JKXXAF JP 02126241 A2 19900515 Heisei).
- Mitsuya M, Suzuki T, Koyama T, Shirai H, Taniguchi Y, Satsuki M, Suga S (2000) Bright red organic light-emitting diodes doped with a fluorescent dye. *Appl Phys Lett* 77:3272–3275
- Fujiwara M, Ishida N, Satsuki M, Suga S (2002) Investigation of blue dopant used coumarin derivatives. *J Photopolym Sci Technol* 2:237–238
- Tang CW, VanSlyke SA, Chen CH (1989) Electroluminescence of doped organic thin films. *J Appl Phys* 65:3610–3616
- Yu TZ, Zhang P, Zhao YL, Zhang H, Meng J, Fan DW, Chen LL, Qiu YQ (2010) Synthesis, crystal structure and photo- and electroluminescence of the coumarin derivatives with benzotriazole moiety. *Org Electron* 11:41–49
- Raju BB, Varadarajan TS (1995) Photophysical properties and energy transfer dye laser characteristics of 7-diethylamino-3-heteroaryl coumarin in solution. *Laser Chem* 16:109–120

24. Griffiths J, Millar V, Bahra GS (1995) The influence of chain length and electron acceptor residues in 3-substituted 7-*N,N*-diethylaminocoumarin dyes. *Dyes Pigments* 28:327–339
25. Kitamura N, Fukagawa T, Kohtani S, Kitoh S, Kunimoto KK, Nakagaki R (2007) Synthesis, absorption, and fluorescence properties and crystal structures of 7-aminocoumarin derivatives. *J Photochem Photobiol A: Chem* 188:378–386
26. Yu TZ, Zhao YL, Ding XS, Fan DW, Qian L, Dong WK (2007) Synthesis, crystal structure and photoluminescent behaviors of 3-(1H-benzotriazol-1-yl)-4-methyl-benzo[7, 8]coumarin. *J Photochem Photobiol A: Chem* 188:245–251
27. Yu TZ, Zhang P, Zhao YL, Zhang H, Meng J, Fan DW (2009) Synthesis, characterization and high-efficiency blue electroluminescence based on coumarin derivatives of 7-diethylaminocoumarin-3-carboxamide. *Org Electron* 10:653–660
28. Zhang H, Yu TZ, Zhao YL, Fan DW, Xia YJ, Zhang P, Qiu YQ, Chen LL (2010) Synthesis, crystal structure and photoluminescence of 3-(4-(anthracen-10-yl)phenyl)-benzo[5,6]coumarin. *spectrochim. Acta Part A* 75:325–329
29. Ye FF, Gao JR, Sheng WJ, Jia JH (2008) One-pot synthesis of coumarin derivatives. *Dyes Pigments* 77:556–558
30. Kaholek M, Hrdlovič P (1999) Characteristics of the excited states of 3-substituted coumarin derivatives and transfer of electronic energy to N-oxyl radicals. *J Photochem Photobiol A: Chem* 127:45–55
31. Kozyra KA, Heldt JR, Diehl HA, Heldt J (2002) Electronic energy transfer efficiency of mixed solutions of the donor–acceptor pairs: coumarin derivatives—acridine orange. *J Photochem Photobiol A: Chem* 152:199–205
32. Li MT, Li WL, Su WM, Zang FX, Chu B, Xin Q, Bi DF, Li B, Yu TZ (2008) High efficiency and color saturated blue electroluminescence by using 4,4'-bis[N-(1-naphthyl)-N-phenylamino]biphenyl as the thinner host and hole-transporter. *Solid State Electron* 52:121–125